energies

Article

Heat Transfer Enhancement in Cooling Jacket of Liquid Cooled Spark Ignition Engine

Faisal Mehmood [1], Hussain Ahmed Tariq [1], Muhammad Anwar [1,*], Hassan Elahi [2], Muhammad Raheel Bhutta [3,*], Talha Irfan Khan [1], Asif Israr [1], Muhammad Umer [1], Usama Waleed Qazi [1] and Usman Ghafoor [1,4]

1 Department of Mechanical Engineering, Institute of Space Technology, Islamabad 44000, Pakistan
2 Department of Mechatronics Engineering, College of Electrical and Mechanical Engineering, National University of Science and Technology, Islamabad 44000, Pakistan
3 Department of Electrical and Computer Engineering, University of UTAH Asia Campus, Incheon 21985, Republic of Korea
4 School of Mechanical Engineering, Pusan National University, Busan 46241, Republic of Korea
* Correspondence: manwar18@gmail.com (M.A.); raheel.bhutta@utah.edu (M.R.B.)

Abstract: Thermal stresses due to long running of spark ignition engine often results in wear and tear of cylinder near the top dead center (TDC). These high thermal stresses at TDC arise due to the high temperature gradient during spark ignition. This situation eventually decreases the life and efficiency of an engine. In this study, the numerical and analytical analysis was carried out on 1298 cc in line four stroke spark ignition (SI) engine having a power output of 63 kW to drop the peak temperature at TDC. to reduce the peak value of temperature, square pin fins were used on the surface of engine cylinder wall near TDC. A parametric study is performed to get an optimal solution for removal of the peak temperature load at TDC. The results showed that the fins with dimension of $4 \times 4 \times 4$ mm^3 along with uniform spacing of 2 mm provide the optimum solution. It has been observed that the peak temperature at TDC dropped down considerably from 160 °C to 133 °C (a percentage reduction of 16.87%) for the pin fins case as compared to without the fin case. Furthermore, the heat transfer effectiveness for the optimum case was calculated as 3.32, whereas for numerical and analytical study it was calculated as 3.43. The error recorded between both the values was limited to 3.2%.

Keywords: pin fins; heat transfer effectiveness; conjugate heat transfer; cooling jacket; spark ignition engine

check for updates

Citation: Mehmood, F.; Tariq, H.A.; Anwar, M.; Elahi, H.; Bhutta, M.R.; Khan, T.I.; Israr, A.; Umer, M.; Qazi, U.W.; Ghafoor, U. Heat Transfer Enhancement in Cooling Jacket of Liquid Cooled Spark Ignition Engine. *Energies* **2023**, *16*, 5126. https://doi.org/10.3390/en16135126

Academic Editors: Davide Di Battista, Fabio Fatigati and Marco Di Bartolomeo

Received: 21 March 2023
Revised: 6 May 2023
Accepted: 26 June 2023
Published: 3 July 2023

1. Introduction

In the past few decades, the automobile industry has grown exponentially and is still progressing day by day. For efficient engine operation, it is essential to run an engine within standard operating temperature range. Over the period of time, different cooling systems have been introduced to enhance cooling characteristics as per the environmental conditions. However, this temperature distribution remains uneven inside the cylinder block. The top dead center (TDC) becomes hotter during combustion strokes as compared to the bottom dead center (BDC). this situation results in the thermal stresses due to cyclic heat load and eventually effect the material at the TDC. This can be minimized by reducing the peak temperature load from TDC. One way to reduce this peak temperature load is to enhance the heat transfer rate at TDC from the engine block to the coolant by introducing the fins at the coolant side. These extended fins increase the contact area with the fluid which results in greater forced convection.

Several studies demonstrated the use of pin fins in different applications for the enhancement of the heat transfer rate. Wei et al. [1] investigated heat transfer characteristics of heat recovery unit numerically. Heat transfer performance of the finned tube was found to be greater as compared to smooth tubes. Serge et al. [2] performed analytical and numerical calculations to optimize the finned heat exchanger. Heat transfer efficiency was found greater using finned surfaces. Tian et al. [3] examined numerically the staggered circular pin finned tube. They found positive thermal hydraulic performance of fin length, fin diameter and number of fins. Lemouedda et al. [4] investigated the performance of serrated finned tube heat exchanger numerically. The main investigation was carried for serrated fins, serrated twisted fins, and number of serrated fins in comparison without fin. Piotr Wais [5] investigated numerically the fin tube heat exchanger with different fin thickness. Singh et al. [6] performed numerical study to investigate the heat transfer and pressure loss characteristics by varying fin geometries. Three different cross sections (rectangular, trapezoidal and triangular) were used for fin geometry. Ali and Briggs [7] performed experimental study for condensation of ethylene glycol by using pin fin tubes. Effect of circumferential pin fin spacing and its thickness was studied. A. Briggs [8] performed experiments on the condensation of R-113 and steam by the introduction of pin fin tubes. Enhancement in heat transfer co-efficient on vapor side was noted to be 3.6 and 9.9 for R-113 and between 2.4 and 2.9 for steam in comparison with plain tube.

O.N. Sara [9] analyzed square pin fins with varying cross-sections in staggered and in line arrangement. The results showed enhancement in heat transfer via square pin finned. Zia Ud din et al. [10] numerically investigates the performance of moving longitudinal and exponential fins with variable thermal conductivity, thermal emissivity, and heat transfer coefficient. Their findings indicate that the exponential fin exhibits higher heat transfer rates compared to the trapezoidal fin. Wei et al. [11] carried out experiments on a silicon chip dipped in a pool of gas dissolved FC-72. Square micro pinned fins of six varying dimensions were introduced to enhance heat flux from the silicon chips. The results revealed considerable increment in heat flux with a maximum increase of 4.2 times as compared to the smooth silicon chip. Chyu and Hsing [12] analyzed experimentally pin fins with a variation in array configuration and cross-section area. Results showed that square pin fins equipped with better heat transfer as compared to diamond and circular pin fins. Peltonen et al. [13] performed numerical and experimental study of plate and pin fin heat exchangers. Results revealed that due to localized vortex shedding, rate of heat transfer for pin fins increased twice as compared to the planar fins. Jeng and Tzeng [14] performed experiments to analyze pressure drop and rate of heat transfer by introducing square and circular pin fins inside rectangular duct with staggered and in-line fin arrangement. The in-line square pin fin array proved to have lower pressure drop and higher heat transfer as compared to circular pin fins. E. M. A. Mokheimer [15] evaluated the performance of annular fins with various profiles.

Saha and Acharya [16] performed numerical analysis for heat transfer characteristics in a channel with an array of cubical pin fins. With the introduction of pin fins, rate of heat transfer observed twice as compared to the smooth duct. Tariq et al. investigated the conjugate heat transfer problem for cellular structures using air [17], water [18], and Al_2O_3-H_2O, CuO-H_2O nano-fluids [19]. Anwar et al. [20] performed numerical calculation to analyse mini channel heat sink using CuO-H_2O nano-fluids as a coolant. Xie et al. [21] studied numerically the heat transfer and pressure drop characteristics of mini channel heat sink. Tariq et al. [22] investigated the effect of slab thickness in miniature devices.

It has been observed that pin fins have been extensively used for heat transfer enhancement in different applications. Pin fins may have also been utilized to enhance the heat transfer inside the engine. Hitachi et al. [23] performed numerical analysis to optimize the liquid cooling performance of automotive compact insulate gate bipolar transistor (IGBT) module. Square fins were preferred over round fins due to their outstanding heat dissipation and velocity flow performance. Selim et al. [24] performedan experimental study to increase heat transfer by introducing the fins inside the coolant passages of cylinder head. Heat transfer coefficient was enhanced up to 180%. The effect of fin length, number of fins, and fins material were studied. A review paper by Bhattad et al. [25] examined the hydrothermal performance of heat exchangers used in engine applications, when utilizing mono/hybrid nanofluids. A review study by Sachar et al. [26] provide insights of certain alterations in material, type, design, number of fins, and other parameters that can improve the efficiency of fins and further enhance the performance of engines. Rao et al. [27] investigated the use of aluminum alloy 6061, A204, and Magnesium alloy for rectangular and circular fins with thicknesses of 2.5 mm and 3 mm. A comparison using Pro-E and ANSYS 16.0 software revealed that, reducing the fin thickness and utilizing circular fins resulted in increased efficiency and effectiveness of the fins.

As evident from the literature, the addition of pin fins has a significant impact on heat transfer. However, taking the benefits of adding pin fins on the periphery of cylinder can reduce the peak temperature load which needed to be addressed. In this context, this study aimed to minimize the peak temperature load at TDC by enhancing heat transfer rate while introducing square pin fins on coolant side cylinder wall. We performed detailed parametric investigation to obtain optimal parameters for square pin fins. The square pin fins of varying cross-sectional area, fin height, fin width and fin spacing have been numerically analyzed and compared. Finally, we compared the results for optimal design with the analytical results and found the percentage error between them.

2. Analytical Analysis

The analysis was carried out on 1298cc in line four stroke Spark Ignition (SI) Engine having power output of 63 kW, bore of 74 mm and stroke of 75.5 mm, its thermal resistance circuit is shown in Figure 1 and its cylindrical block in Figure 2. Cylinder block and sleeve was made up of aluminum alloy T6 and cast iron, respectively. Thermal conductivity of aluminum alloy T6 and cast iron were taken as 109 W/mK and 46 W/mK, respectively. The water flow rate in the engine was considered constant as 12LPM (2.57 m/s) when the engine was revolving at 1500 rpm. The inner and outer radius of sleeve was 37 mm and 39.5 mm, respectively. The coolant moves in annulus between radii of 45 mm to 53.5 mm. The peripheral length where fins were installed was 32.76 mm. Sleeve, cylinder block and water are shown by red, grey and blue spectrum, respectively, in the thermal circuit diagram Figure 1. The properties of block and sleep are provided in Table 1.

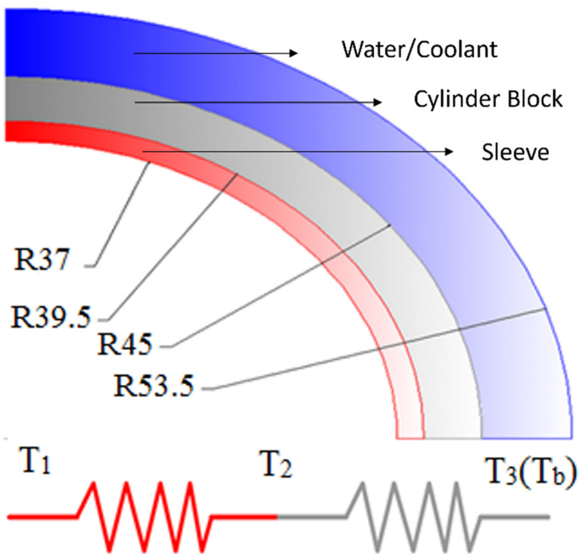

Figure 1. Thermal circuit diagram.

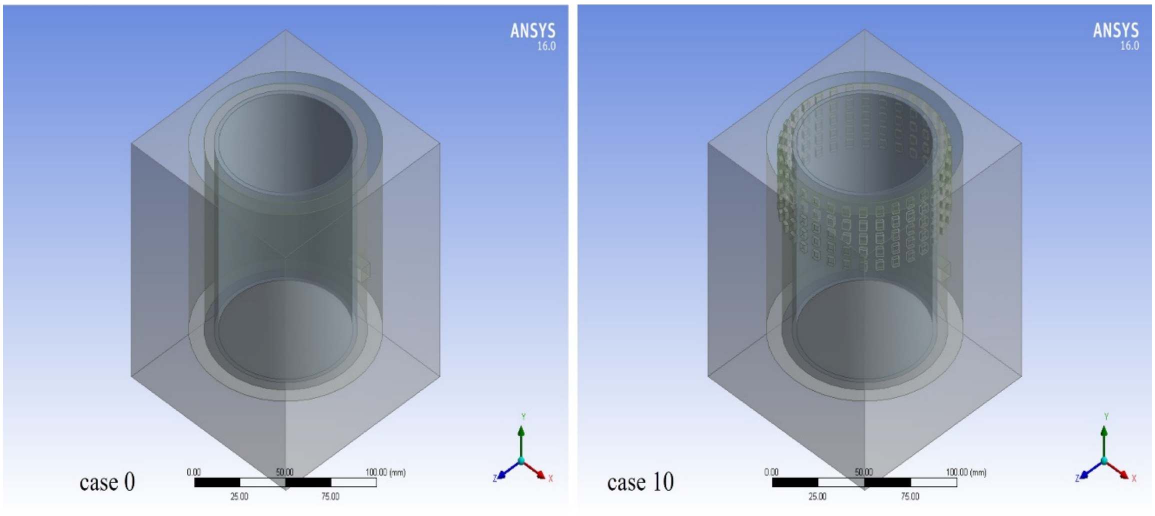

Figure 2. Model of cylindrical block.

Table 1. Properties of engine block and sleeve.

Part Detail	Material	Density (Kg/m^3)	Thermal Conductivity (W/m K)	Specific Heat Constant (KJ/Kg K)
Block	Aluminum Alloy T6	2768	109	0.896
Sleeve	Gray Cast Iron	7200	46	0.46

Following assumptions were considered for the analytical analysis.

1. Flow is steady
2. Fin spacing is uniform in the longitudinal as well as in horizontal direction
3. One cylinder is assumed for the sake of simplicity
4. Heat transferred to the surrounding by the engine is 35% [28]

Data Reduction

We adopt the following procedure for data reduction as:

Heat supplied to the engine was calculated using Equation (1) taken from [29],

$$Thermal\ Efficiency = \eta_{th} = \frac{W_{out}}{Q_{in}} \tag{1}$$

Thermal resistance that encounters the flow of heat through the cylinder wall was calculated using Equation (2) taken from [29],

$$\mathrm{Rth} = \ln(\mathrm{r_o}/\mathrm{r_i})/2\Pi \mathrm{kl} \tag{2}$$

Temperature of coolant side cylinder wall i.e., base temperature 'T_b' at TDC as shown in Figure 1 was calculated using Equation (3) taken from [29],

$$Heat\ transfer\ through\ wall = \dot{Q}_{wall} = \frac{T_1 - T_b}{R_{th}} \tag{3}$$

Reynolds number and Prandtl number for the fluid flowing across the circular annulus having pin fins was calculated from Equation (4) and Equation (5), respectively, taken from [29],

$$Reynoldnumber = R_E = \frac{VD_h}{v} \tag{4}$$

$$Prandtlnumber = P_r = \frac{\mu C_p}{K} \tag{5}$$

Convective heat transfer coefficient was calculated from Equation (6) taken from [29],

$$h_c = \pi r^2 = \frac{kNu}{D_h} \tag{6}$$

Fin efficiency was calculated from Figure 1b in Ref. [15] using empirical relations given in Equations (7) and (8) as:

$$m = h\sqrt{\frac{h_u + h_l}{k_s w}} \tag{7}$$

$$R_{ratio} = r_o / r_i \tag{8}$$

Heat transferred trough pin finned was calculated from Equation (9) taken from [29],

$$\dot{Q}_{fin} = \eta_{fin} Q_{finmaximum} \tag{9}$$

Rate of heat transfer from pin finned surface was calculated from Equation (10) taken from [29],

$$\dot{Q}_{fin} = \eta_{fin} h A_{fin} (T_b - T_\infty) \tag{10}$$

Heat transferred through un-finned surface was calculated from Equation (11) taken from [29],

$$\dot{Q}_{Unfin} = h A_{Unfin} (T_b - T_\infty) \tag{11}$$

Gross rate of heat transfer was calculated from Equation (12) taken from [29],

$$\dot{Q}_T = \dot{Q}_{fin} + \dot{Q}_{Unfin} \tag{12}$$

Heat transfer without fins was calculated from Equation (13) taken from [29],

$$\dot{Q}_{NoFin} = h_c A_{nofin} (T_b - T_\infty) \tag{13}$$

Fin effectiveness was calculated from Equation (14) taken from [29],

$$\varepsilon_{fin} = \frac{Q_T}{Q_{NoFin}} \tag{14}$$

3. Numerical Analysis

We utilized the computational fluid dynamics (CFD) approach to vitalize the conjugate heat transfer problem. We used an ANSYS design modeler for modelling of geometry according to dimensions, ANSYS meshing for CFD mesh and ANSYS fluent as a CFD solver. ANSYS 16.0 commercial software was used to solve conservation equations from (15)–(19) [21,30]. Pressure based solver, absolute velocity formulation, and transport equation for Realizable k-ε model were used. Pressure and velocity coupling were controlled by a semi-implicit method for pressure-linked equations (SIMPLE). A second-order spatial discretization scheme was used for the pressure while for the discretization of momentum, turbulent kinetic energy and turbulent dissipation rate second order upwind scheme was used. Heat transfer connection was set from cast iron sleeve to aluminum alloy block, and then from aluminum block to water. To evaluate thermal and flow characteristics in numerical study, the following assumptions were used:

- The flow is incompressible, turbulent, 3D and in steady state
- Fluid thermal properties are considered constant throughout the flow
- There is no heat generation inside the structure and no viscous heating

Governing equations on the basis of above assumptions are as follows for conservation of mass, momentum, energy, turbulence kinetic energy and turbulence dissipation rate:

For conservation of mass [30]

$$\frac{\partial}{\partial x_i}(\rho u_i) = 0 \tag{15}$$

For conservation of momentum [30]

$$\frac{\partial}{\partial x_i}\left(\rho u_i u_j\right) = -\frac{\partial p}{\partial x_j} + \frac{\partial}{\partial x_i}\left[(\mu + \mu_t)\frac{\partial \mu_j}{\partial x_i}\right] + \frac{\partial}{\partial x_i}\left[(\mu + \mu_t)\frac{\partial \mu_i}{\partial x_j}\right] \quad \text{where } j = 1,2,3 \tag{16}$$

For conservation of energy [30]

$$\frac{\partial}{\partial x_i}(\rho u_i T) = \frac{\partial}{\partial x_i}\left[\left(\frac{\lambda}{c_p} + \frac{\mu_t}{\sigma_T}\right)\frac{\partial T}{\partial x_i}\right] \tag{17}$$

For conservation of turbulence kinetic energy (k) [30]

$$\frac{\partial}{\partial x_i}(\rho k u_i) = \frac{\partial}{\partial x_i}\left[\left(\mu + \frac{\mu_t}{\sigma_k}\right)\frac{\partial k}{\partial x_i}\right] + G_k - \rho\varepsilon \tag{18}$$

For conservation of turbulence dissipation rate (ε) [30]

$$\frac{\partial}{\partial x_i}(\rho\varepsilon u_i) = \frac{\partial}{\partial x_i}\left[\left(\mu + \frac{\mu_t}{\sigma_\varepsilon}\right)\frac{\partial \varepsilon}{\partial x_i}\right] + \frac{\varepsilon}{k}(c_1 G_k - c_2\rho\varepsilon) \tag{19}$$

G_k is generation of turbulence kinetic energy which can be described as

$$G_k = -\rho\overline{u_i' u_j'}\frac{\partial u_j}{\partial x_i} \tag{20}$$

μ_t is turbulent viscosity and is described as

$$\mu_t = \frac{\rho C_\mu k^2}{\varepsilon} \tag{21}$$

C_μ is described as

$$C_\mu = 1/\left[A_o + \left(\frac{A_s k U^*}{\varepsilon}\right)\right] \tag{22}$$

A_s is described as

$$A_s = \sqrt{6}cos\varnothing \tag{23}$$

where $C_2 = 1.9$, $\sigma_k = 1$, $\sigma_\varepsilon = 1.2$, $A_o = 4.04$ are constants

The following boundary conditions were used for numerical study as:

- Flow inlet velocity as 2.57 m/s
- Pressure outlet at 0 gauge
- Cast iron sleeve inner wall temperature is kept constant at 185 °C [28]
- Incoming flow is assumed at ambient 300 K temperature

3.1. Mesh Independent Study

Mesh was considered to be independent when the temperature difference shows no more than 1% of deviation with the number of elements. Results were examined for the temperature difference between water inlet temperature and sleeve inner cylinder wall temperature with varying number of elements. Once the number of elements crossed 7 million, a negligible temperature difference was observed. Therefore, the minimum threshold was set to 7 million for the whole parametric study. Variation of temperature difference versus the number of elements is described in Figure 3.

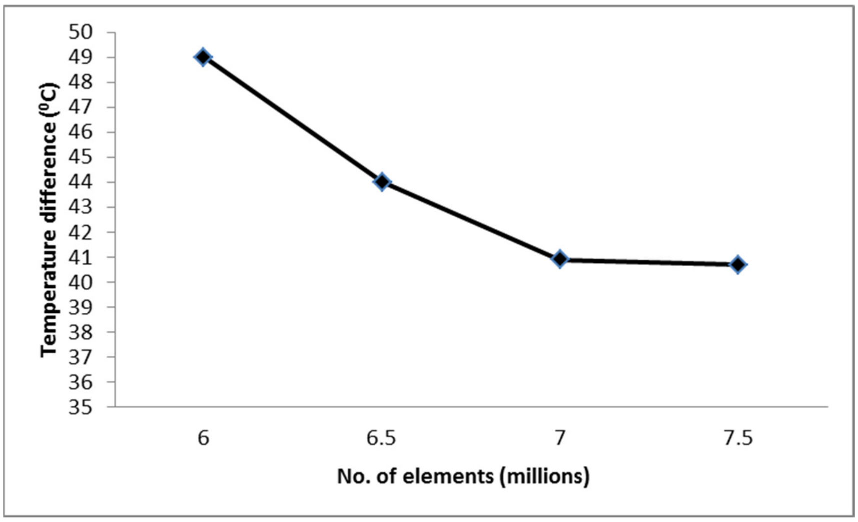

Figure 3. Mesh independent study.

3.2. Parametric Study

In this section, parameters of square pin fins were varied and discussed in detail. The scheme followed the effect of fin cross-section, effect of fin spacing and effect of height to compute fin effectiveness for each case. An optimal structure was evaluated after detailed parametric study. A single cylinder was considered for the ease of numerical analysis. Square pin fins were introduced in the passage of coolant jacket to enhance rate of heat transfer. Ten cases were studied (i.e., from case-1 to case-10) while a no fin case was assumed as case-0. The isometric view of cylinder block is shown in Figure 4.

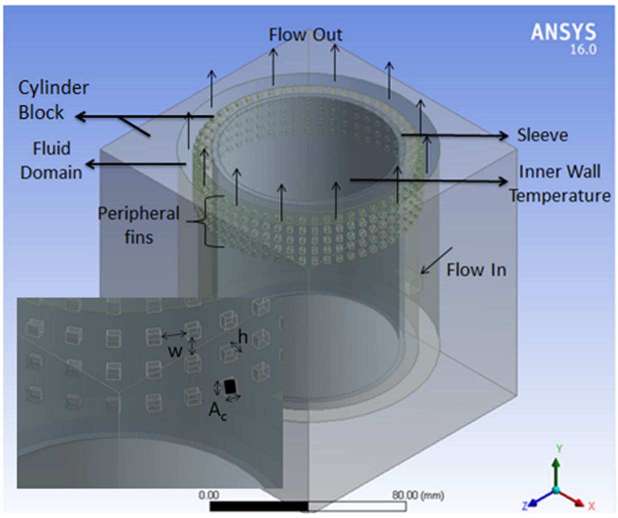

Figure 4. Cylinder block isometric view.

3.2.1. Effect of fin Cross-Section Area

In this section, three cases were analyzed by changing the cross-section area of square pin fins from case-1 to case-3, while keeping the fin spacing and fin height constant. Geometric dimensions are given in Table 2.

Table 2. Fin dimensions.

	Fin Cross Section A_c (mm^2)	Fin Spacing w (mm)	Fin Height h (mm)
Case-1	4	3	2
Case-2	9	3	2
Case-3	16	3	2

Case-3 was proven to be the optimal solution having cross section of 0.0153 m^2 with fin effectiveness of 1.67 followed by case-2 and case-1 with the fin effectiveness of 1.57 and 1.41, respectively. The details of the results are given in Table 3.

Table 3. Effect of fin cross-section comparison.

	Total Surface Area A_s (m^2)	Fin Cross-Section Area A_c (mm^2)	Heat Transfer without Fin $\dot{Q}$ (W)	Heat Transfer with Fin $\dot{Q}$ (W)	Fin Effectiveness ε_{fin}
Case-1	0.0131	4	185.58	262.51	1.41
Case-2	0.0148	9	185.58	291.91	1.57
Case-3	0.0153	16	185.58	306.47	1.65

3.2.2. Effect of Fin Spacing

In this section, the effect of fin spacing is studied with constant fin cross-section area and fin height. Four cases were studied from case-4 to case-7 to obtain optimized fin spacing. Geometric dimensions are given in Table 4.

Table 4. Effects of fin spacing.

	Fin Cross Section A_c (mm^2)	Fin Spacing w (mm)	Fin Height h (mm)
Case 4	16	2	2
Case 5	16	3	2
Case 6	16	4	2
Case 7	16	5	2

Case-4 was proven to be the best solution having fin spacing of 2 mm with fin effectiveness of 1.72 followed by case-5, case-6, and case-7 with the fin effectiveness of 1.64, 1.46, and 1.28, respectively. The detailed results are given in Table 5.

Table 5. Effect of fin spacing comparison.

	Total Surface Area A_s (m^2)	Fin Spacing w (mm)	Heat Transfer without Fin $\dot{Q}$ (W)	Heat Transfer with Fin $\dot{Q}$ (W)	Fin Effectiveness ε_{fin}
Case-4	0.0112	2	185.58	319.34	1.72
Case-5	0.0156	3	185.58	305.57	1.64
Case-6	0.0137	4	185.58	271.32	1.46
Case-7	0.0112	5	185.58	238.60	1.28

3.2.3. Effect of fin height

In this section, the effect of fin height is studied by keeping the fin cross-section area and fin spacing constant. Geometric dimensions from case-8 to case-10 are given in Table 6.

Table 6. Effects of fin height.

	Fin Cross Section A_c (mm^2)	Fin Spacing w (mm)	Fin Height h (mm)
Case-8	16	2	2
Case-9	16	2	3
Case-10	16	2	4

Case-10 with fin height of 4 mm proved to be best case with a fin effectiveness of 3.43 followed by case-9 and case-8 with a fin effectiveness of 2.91 and 1.72, respectively. The red region shows the hotter inner side of sleeve while blue color shows the temperature contour at coolant side in Figure 5. The detailed results are given in Table 7.

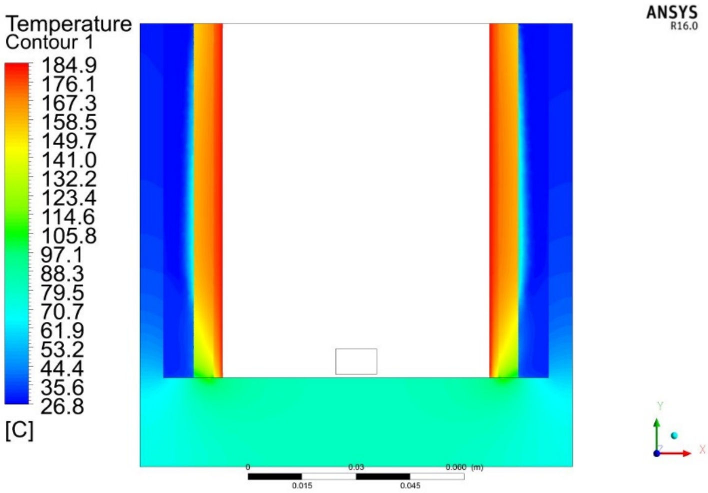

Figure 5. Simulation results with no fins (Case-0).

Table 7. Effect of fin height comparison.

	Total Surface Area A_s (m^2)	Fin Height h (mm)	Heat Transfer without Fin $\dot{Q}$ (W)	Heat Transfer with Fin $\dot{Q}$ (W)	Fin Effectiveness ε_{fin}
Case-8	0.0167	2	185.58	319.34	1.72
Case-9	0.0205	3	185.58	540.23	2.91
Case-10	0.0238	4	185.58	638.30	3.43

4. Results and Discussions

4.1. Effect of Pressure Drop

The effect of pressure drop with surface area is shown in Figure 6. With an increase in surface area using fin surfaces, the pressure drop gradually increases. More fins eventually shorten the fin spacing which allows the coolant to pass through them. This in fact causes the blockage in the flow and results in increased pressure drop across inlet to outlet. Minimum pressure drop was observed for case-1 464 Pa while the maximum pressure drop was observed for case-9 as 573 Pa in comparison to no-fin case-0.

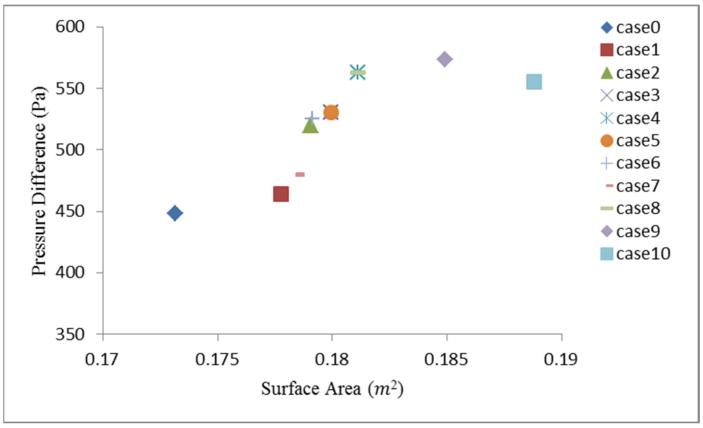

Figure 6. Variation of pressure drop with surface area.

4.2. Temperature Distribution across the Wall

Within an internal combustion engine (IC Engine), the combustion of the air-fuel mixture generates temperatures that can rise as high as 2000 °C, posing the risk of melting the cylinder body and engine head. Inadequate cooling can result in the combustion of lubricating oil, leading to engine part seizure and damage to oil rings and compression rings [31]. The addition of fins shows a significant reduction in internal temperature. Temperature distribution across the wall at TDC is shown in Figure 7. The location of five different points P_1, P_2, P_3, P_4, and P_5 at vicinity are shown in Figure 8. The inner wall temperature of sleeve was kept constant as 185 °C. The temperature gradually decreases starting from the sleeve inner side up to cylinder outer wall surface. It is evident from the results that for case-0 with no fin, the temperature drop is from 185 °C to 159.6 °C, while for the case-10, maximum temperature drop was observed (i.e., from 185 °C to 133 °C). Maximum and minimum drop in temperature was measured as 26.6 °C and 14.9 °C, respectively, in comparison to case-0.

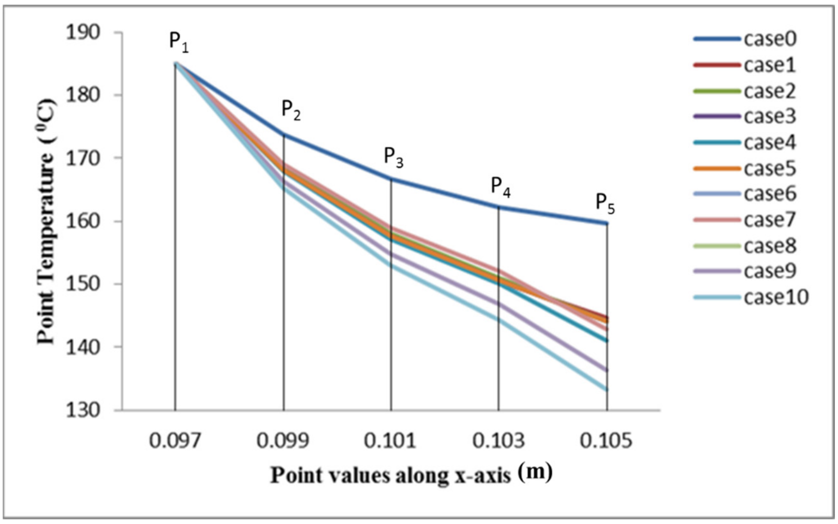

Figure 7. Temperature distribution across the wall at TDC.

Temperature contour of inner side of cylinder block made of aluminum alloy for case-0 and case-10 is shown in Figure 9. It can be clearly observed that temperature drops from red color (which is high) for case-0 to orange color for case 10 at TDC. This clearly signifies the importance of adding fins on top periphery of cylinder. Peak temperature value drops using pin fins as compared to no fin, which will further result in reduction of thermal stresses on TDC.

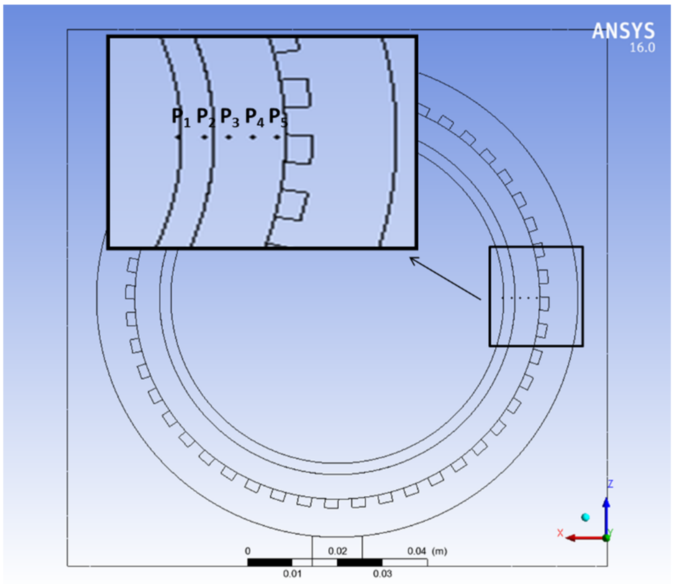

Figure 8. Points location along *x*-axis across the wall.

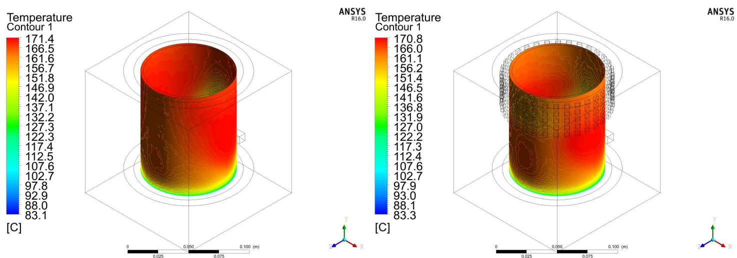

Figure 9. Temperature contour of cylinder block inner side; **Left** case-0, **Right** case-10.

4.3. Effect of Surface Area on Heat Transfer Rate

The effect of heat transfer rate with surface area is shown in Figure 10. With increase in surface area using finned surfaces, the rate of heat transfer increases gradually. Case-0 represents a minimal rate of heat transfer with respect to other cases. Case-4 and case-5 show a reasonable enhancement of rate of heat transfer as surface area increases. Case-8 and case-9 provide a fair increment in the rate of heat transfer. Maximum and minimum heat transfer rate was recorded for case-10 and case-7, respectively.

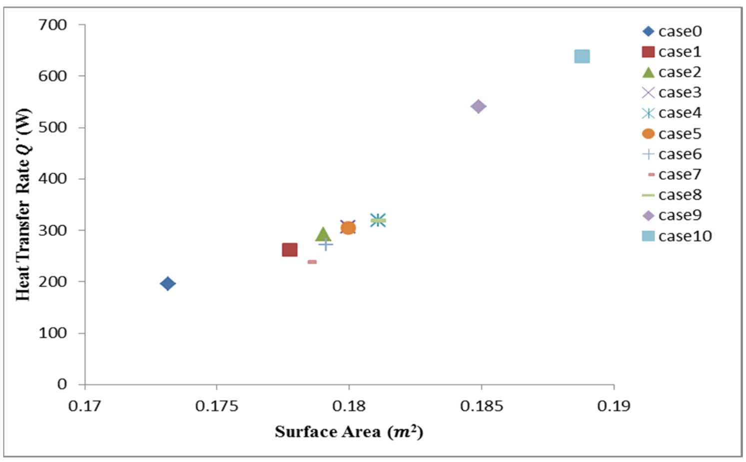

Figure 10. Variation of heat transfer rate with surface area.

4.4. Fin Effectiveness

The fin effectiveness plays a significant role in finding the performance of fins utilized, as compared with a no fin surface area. Analytical and numerical data of fin effectiveness for the optimal case i.e., case-10 is shown in Figure 11. The effectiveness of the case-10 was recorded as 3.32 and 3.43 analytically and numerically, respectively. Certainly, the rate of heat transfer is improved as the effectiveness of case-10 is greater than 1. The error recorded between analytical and numerical results was 3.2%.

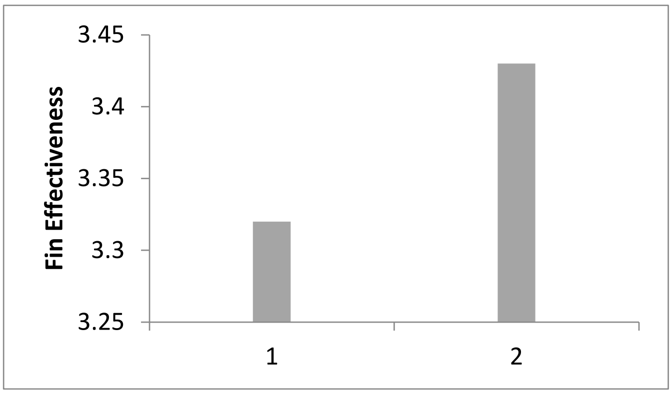

Figure 11. Fin Effectiveness (1: Analytically, 2: Numerically).

5. Conclusions

The temperatures generated due to the combustion of the air-fuel mixture within an internal combustion engine (IC engine) can reach up to 2000 °C, which can affect the cylinder body and engine head (as they may melt). If the cooling system is not sufficient, the lubricating oil can ignite and cause damage to the engine parts, such as oil rings and compression rings, resulting in seizure. In this study, we investigated the effect of square pin fins on heat transfer to reduce the peak temperature load at TDC. The maximum pressure drop was observed for case-10 due to a greater area which creates hindrance for the flow, while better minimum pressure drop was offered by case-1 in comparison to case-0. The base temperature dropped down from 160 °C (case-0) to 133 °C (case-10), which is 16.87% lower as compared to case-0. The heat transfer effectiveness for case-10 was found to be 3.32 and 3.43 for the analytical and numerical data, respectively. The error noted between both the values was 3.2%, predicting the significance of the numerical study. A significant drop in peak temperature load was observed for the case-10 when compared with no fin case-0, demonstrating the value of this study. Case-10 was found to be the best among all other cases studied in this work.

Author Contributions: Methodology, H.A.T., H.E., M.R.B., T.I.K. and M.U.; Software, F.M.; Formal analysis, M.A. and T.I.K.; Investigation, F.M. and H.A.T.; Resources, H.E.; Data curation, M.R.B.; Writing—original draft, M.A., A.I. and U.G.; Writing—review & editing, M.A., A.I., U.W.Q. and U.G.; Visualization, M.U. and U.W.Q.; Supervision, M.A.; Project administration, M.R.B.; Funding acquisition, M.R.B. All authors have read and agreed to the published version of the manuscript.

Funding: This work was supported by the National Research Foundation (NRF) of Korea through the Auspices of the Ministry of Science and ICT, Republic of Korea, under Grant NRF-2020R1G1A1012741.

Data Availability Statement: No supporting data required.

Conflicts of Interest: The authors declare no conflict of interest.

Nomenclature

A_s	Surface Area of heat transfer surface, mm^2
A_{fin}	Surface Area of introduced fins, mm^2

$A_{un\text{-}fin}$	Surface area leftover by fins, mm^2
A_c	Cross-section area of fin
C_p	Specific heat, kJ/kgK
$\dot{m}$	Mass flow rate, kg/s
ΔP	Pressure Difference, Pa
$\dot{Q}$	Heat transfer rate, W
$\dot{Q}_{fin}$	Heat transfer rate through introduced fins, W
$\dot{Q}_{unfin}$	Heat transferred left over by the fins, W
$\dot{Q}_T$	Combined heat transfer through fin and finned surface, W
$\dot{Q}_{nofin}$	Heat transfer without fins, W
Q	Volumetric flow rate, m^3/s
R_{th}	Thermal resistance, °C/W
T	Temperature (°C)
T_b	Base temperature of the surface where fins are attached, (°C)
T_∞	Fluid Inlet Temperature, °C
T_o	Fluid Outlet Temperature, °C
t	Wall thickness, mm
u,v,w	Velocity in x,y,z, respectively (m/s)
h_u	Convective heat transfer coefficient for upper surface, W/m^2 K
h_l	Convective heat transfer coefficient for lower surface, W/m^2 K
m	Dimensionless parameter
k_s	Thermal conductivity of fin, W/mK
R_{ratio}	Radius ratio
r_o	outer diameter, mm
r_i	inner diameter, mm
R_E	Reynolds number
D_h	Hydraulic diameter, mm
ν	Kinematic viscosity,
Pr	Prandtl number
μ	Dynamic viscosity
k	Thermal conductivity, W/mK
K	Thermal diffusivity
h_c	Convective heat transfer coefficient, W/m^2 K
h	Fin height, mm
w	Fin width, mm
LPM	Litres per minute
ε_{fin}	Fin effectiveness
W_{out}	Output of the engine produced, W
Q_{in}	Heat supplied to the engine, W
Greek symbol	
α_{sf}	Surface area density
ϱ	Density (kg/m^3)
μ_t	Turbulence viscosity (kg/ms)

References

1. Wei, L.; Zhu, G.; Jin, Z. Numerical Simulation of Heat Transfer in Finned Tube of Heat Recovery Unit Using Fluid-Solid Coupled Method. *Adv. Mech. Eng.* **2014**, *7*, 127815. [CrossRef]
2. Serge, N.N.; Tang, F.; Zhang, Z.X. An optimization study on the finned tube heat exchanger used in hydride hydrogen storage system—Analytical method and numerical simulation. *Int. J. Hydrogen Energy* **2012**, *37*, 16078–16092.
3. Tian, E.; He, Y.; Tao, W. Numerical Simulation of Finned Tube Bank Across a Staggered Circular-Pin-Finned Tube Bundle. *Numer. Heat Transf. Appl.* **2015**, *68*, 737–760. [CrossRef]
4. Lemouedda, A.; Schmid, A.; Franz, E.; Breuer, M.; Delgado, A. Numerical investigations for the optimization of serrated finned-tube heat exchangers. *Appl. Therm. Eng.* **2011**, *31*, 1393–1401. [CrossRef]
5. Wais, P. Correlation and numerical study of heat transfer for single row cross-flow heat exchangers with different fin thickness. In Proceedings of the IX International Conference on Computational Heat and Mass Transfer, ICCHMT2016, Cracow, Poland, 23–26 May 2016; Volume 157, pp. 177–184.

6. Singh, S.; Sorensen, K.; Condra, T.J. Performance study of a fin and tube heat exchanger with different fin geometry. In Proceedings of the 29th International Conference on Efficiency, Cost, Optimisation, Simulation and Environmental Impact of Energy Systems, Portoroz, Slovenia, 19–23 June 2016.
7. Ali, H.M.; Briggs, A. Condensation of ethylene glycol on pin fin tubes, effects of circumferential pin spacing and thickness. *Appl. Therm. Eng.* **2012**, *49*, 9–13. [CrossRef]
8. Briggs, A. Enhanced condensation of R-113 and steam on three dimensional pin-fin tubes. *Heat Transf.* **2003**, *16*, 61–79. [CrossRef]
9. Sara, O.N. Performance analysis of rectangular ducts with staggered square pin fins. *Energy Conserv. Manag.* **2003**, *44*, 1787–1803. [CrossRef]
10. Din, Z.U.; Ali, A.; Khan, Z.A.; Zaman, G. Investigation of moving trapezoidal and exponential fins with multiple nonlinearities. *Ain Shams Eng. J.* **2023**, *14*, 101959. [CrossRef]
11. Wei, J.J.; Honda, H. Effects of fin geometry on boiling heat transfer from silicon chips with micro pin fins immersed in FC 72. *Int. J. Heat Mass Transf.* **2003**, *46*, 4059–4070. [CrossRef]
12. Chyu, M.K.; Hsing, Y.C.; Natarajan, V. Convective Heat Transfer of Cubic fin arrays in a narrow channel. *ASME J. Turbomach.* **1998**, *120*, 362–367. [CrossRef]
13. Peltonen, P.; Saari, K.; Kukko, K.; Vuorinen, V.; Partanen, J. Large Eddy simulation of local heat transfer in plate and pin fin heat exchangers confined in a pipe flow. *Int. J. Heat Mass Transf.* **2019**, *134*, 641–655. [CrossRef]
14. Jeng, T.M.; Tzeng, S.C. Pressure Drop and Heat Transfer of Square Pin Fin arrays in inline and staggered arrangements. *Int. J. Heat Mass Transf.* **2006**, *50*, 2364–2375. [CrossRef]
15. Mokheimer, E.M.A. Performance of annular fins with different profiles subject to variable heat transfer coefficient. *Int. J. Heat Mass Transf.* **2002**, *45*, 3631–3642. [CrossRef]
16. Saha, A.K.; Acharya, S. Unsteady Simulation of Turbulent flow and heat trransfer in a channel with a periodic array of cubic pin fins. *Numer. Heat Transf. (Part A)* **2004**, *46*, 731–763. [CrossRef]
17. Tariq, H.A.; Israr, A.; Khan, Y.I.; Anwar, M. Numerical and experimental study of cellular structures as a heat dissipation media. *Heat Mass Transf.* **2018**, *55*, 501–511. [CrossRef]
18. Tariq, H.A.; SHOUKAT, A.A.; Anwar, M.; Israr, A.; Ali, H.M. Water Cooled Micro-hole Cellular Structure as a Heat Dissipation Media: An Experimental and Numerical Study. *J. Therm. Sci.* **2018**, *24*, 683–692. [CrossRef]
19. Tariq, H.A.; Shoukat, A.A.; Hassan, M.; Anwar, M. Thermal Management of Microelectronic Devices using Micro-hole Cellular Structure and Nanofluids. *J. Therm. Anal. Calorim.* **2018**, *136*, 2171–2182. [CrossRef]
20. Anwar, M.; Tariq, H.A.; Shoukat, A.A.; Ali, H.M.; Ali, H. Numerical study for heat transfer enhancement using CuO-H_2O nano-fluids through minichannel for microprocessor cooling. *J. Therm. Sci.* **2018**, *24*, 2965–2976. [CrossRef]
21. Xie, X.L.; Tao, W.Q.; He, Y.L. Numerical Study of Turbulent Heat Transfer and Pressure Drop Characteristics in a Water-Cooled Minichannel Heat Sink. *J. Electron. Packag.* **2007**, *129*, 247–255. [CrossRef]
22. Tariq, H.A.; Anwar, M.; Malik, A. Numerical Investigations of Mini-Channel Heat Sink for Microprocessor Cooling: Effect of Slab Thickness. *Arab. J. Sci. Eng.* **2020**, *45*, 5169–5177. [CrossRef]
23. Hitachi, T.; Gohara, H.; Nagaune, F. Direct liquid cooling IGBT Module for automotive applications. In *Fuji Electric Review*; Fuji Electric Co., Ltd.: Hong Kong, China, 2012; pp. 55–59.
24. Selim, M.Y.E.; Elfeky, S.M.S.; Helali, A. Enhancement of Coolant Side Heat Transfer In Water Cooled Engines By Using Finned Cylinder Heads. In Proceedings of the ICEF 2005 ASME Internal Combustion Engine Division 2005 Fall Technical Conference, Ottawa, ON, Canada, 11–14 September 2005; pp. 523–543.
25. Bhattad, A.; Atgur, V.; Rao, B.N.; Banapurmath, N.R.; Yunus Khan, T.M.; Vadlamudi, C.; Krishnappa, S.; Sajjan, A.M.; Shankara, R.P.; Ayachit, N.H. Review on Mono and Hybrid Nanofluids: Preparation, Properties, Investigation, and Applications in IC Engines and Heat Transfer. *Energies* **2023**, *16*, 3189. [CrossRef]
26. Sachar, S.; Parvez, Y.; Khurana, T.; Chaubey, H. Heat transfer enhancement of the air-cooled engine fins through geometrical and material analysis: A review. *Mater. Today Proc.* **2023**, *in press*. [CrossRef]
27. Srinivas, D.; Kumar, T.; Santosh, R.; Suresh, V.; Eshwaraiah, R. Thermal analysis and optimization of engine cylinder fins by varying geometry and material. In Proceedings of the 1st International Conference on Manufacturing, Material Science and Engineering (ICMMSE-2019), Telangana, India, 16–17 August 2019; Volume 8, pp. 404–412.
28. Pulkrabek, W.W. *Engineering Fundamentals of the Internal Combustion Engine*; Prentice Hall: Hoboken, NJ, USA, 2004.
29. Cengel, Y.A. *Heat Transfer, A Practical Approach*, 2nd ed.; McGraw-Hill: New York, NY, USA, 1997.
30. Ansys Fluent Documentation. Theory Guide and User Guide. Release 16.0. Available online: http://www.ansys.com (accessed on 1 January 2015).
31. Choudhary, P.; Sachar, S.; Khurana, T.; Jain, U.; Parvez, Y.; Soni, M. Energy analysis of a single cylinder 4-stroke diesel engine using diesel and diesel-biodiesel blends. *Int. J. Appl. Eng.* **2018**, *13*, 10779–10788.